

Nonreciprocal phase behavior in reflection of electromagnetic waves from magnetic materials

T. Dumelow,* R. E. Camley,[†] Kamsul Abraha,[‡] and D. R. Tilley[§]

Department of Physics, University of Colorado at Colorado Springs, Colorado Springs, Colorado 80933-7150

(Received 16 June 1997)

Most experimental and theoretical treatments of reflection of electromagnetic radiation from magnetic materials have concentrated on the intensity of the reflected and transmitted waves. We point out that the behavior of the phase of these waves can be quite different from the intensity, and that it can have direct experimental consequences. In particular, the reflected intensity from a magnetic material with low damping in the Voigt geometry is reciprocal, i.e., the intensity is the same when the reflected and incident waves are interchanged. In contrast, the phase of the reflected wave is strongly nonreciprocal. This nonreciprocity in phase produces a nonreciprocal intensity in a structure where a dielectric film is placed on an antiferromagnet. We explore the general properties of the phase and amplitude of reflected and transmitted waves in a variety of geometries using the antiferromagnet FeF_2 as an example. General thermodynamic arguments are used to support some of the specific results. [S0163-1829(98)05026-7]

I. INTRODUCTION

One of the most interesting features in the interaction of electromagnetic waves with magnetic materials is that of nonreciprocal¹ reflection. In this effect a simple reversal of the direction of the incident and reflected waves leads to different reflection and transmission coefficients. A series of experimental and theoretical studies of the reflection of infrared radiation from the antiferromagnets MnF_2 (Refs. 2 and 3) and FeF_2 (Refs. 4–7) has recently documented this effect. Nonreciprocal Brillouin light scattering from spin waves in ferromagnetic materials is also quite well known.⁸

To this point nearly all the studies, both experimental and theoretical, have concentrated on the amplitude of the reflected radiation as measured through the intensity. The phase of the waves has been neglected. This is, of course, fairly natural. The intensity is what is typically measured in experiments. In addition, through the use of thermodynamics arguments one can make general arguments connecting the intensity of the incident, reflected, and transmitted light with the absorption of energy in the magnetic material.^{3,9}

An important example of such a thermodynamic result relates to uniaxial antiferromagnets in the presence of an external field. In the Voigt geometry (applied field parallel to the surface and along the uniaxial direction; the incident electromagnetic wave is s polarized and the plane of incidence is perpendicular to the applied field) one can show quite generally that the reflected intensity is reciprocal unless there is some absorption mechanism inside the antiferromagnet.³ If there is absorption, then the reflected wave intensity is nonreciprocal but the transmitted wave intensity is always reciprocal. This asymmetry between the behavior of the intensity of the reflected and transmitted waves is surprising, and illustrates how difficult it is to have good intuition about this problem.

In this paper we concentrate on a new feature of the problem, the nonreciprocal phase of the reflected and transmitted waves. There are a number of reasons for this. First, the phase can behave quite differently from the intensity. For example, when we consider the reflection geometry dis-

cussed in the previous paragraph, the reflected intensity is reciprocal in the absence of damping. In contrast, the phase of the reflected wave can be nonreciprocal even without damping. Second, we note that the nonreciprocal phase of reflected and transmitted waves in layered structures can induce nonreciprocal intensities because of a nonreciprocal interference that occurs. Thus the reflected and transmitted phases have several direct experimental consequences. Third, the phase differences between different transmitted and reflected waves may be measured as we show in Sec. V. Finally, we note that the phase of the reflected and transmitted waves can be a directly measurable quantity. For example, dispersive Fourier-transform spectroscopy can be used to give the relative phase between the incident and reflected beams although this is difficult, as well shall discuss later on.

We know of no thermodynamic arguments that one can use to understand the general behavior of the phase. Thus our approach concentrates on understanding the phase by studying particular examples. In Sec. II we examine reflection and transmission for the s -polarized Voigt geometry described above. This is a particularly important case because there is no mode mixing, i.e., the reflected and transmitted waves are also s polarized. We study several different sample structures. For example, in a semi-infinite antiferromagnet, we find that in the absence of damping the reflected intensity is always reciprocal while the phase is not. For the geometry of a thin dielectric film on a semi-infinite antiferromagnet we find that a nonreciprocal reflected phase that occurs at the dielectric/antiferromagnet interface produces a nonreciprocal net reflection from the structure. In a surprising result, the degree of nonreciprocity oscillates as the thickness of the dielectric film is increased. The period of this oscillation depends on the wavelength of the electromagnetic radiation in the dielectric, and this feature can also be directly connected to the nonreciprocity of the reflected phase at the dielectric/antiferromagnet interface.

In Sec. III we examine a more general geometry, where the plane of incidence is still normal to the surface of the antiferromagnet, but is allowed to be at arbitrary angle with respect to the applied field. In this geometry there is mode

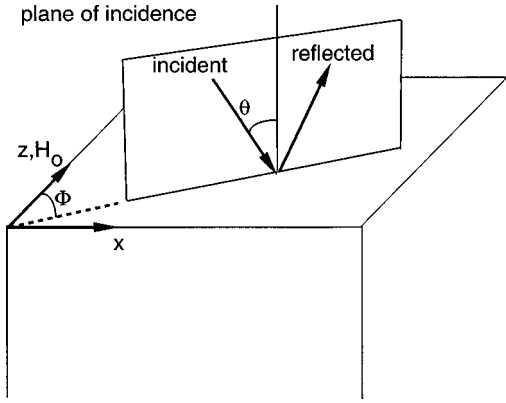


FIG. 1. Reflection geometry considered in this paper. The applied field is along the z axis. The angle of incidence is θ and the angle of the plane of incidence with respect to the field is Φ . The easy axis for the antiferromagnet is also along the z axis.

mixing in that an s -polarized incident wave can lead to both s - and p -polarized reflected and transmitted waves. We establish some general rules about the phase and intensity of both the reflected and transmitted waves.

In Sec. IV we reexamine some thermodynamic arguments connecting nonreciprocal reflection and transmission intensities and absorption within an antiferromagnetic film. An unpolarized incident wave is considered and we derive results connecting the various nonreciprocal transmitted and reflected intensities. These results are used to check the numerical examples in Sec. III. In Sec. V we present methods to measure phase differences between different transmitted and reflected waves.

Finally in Sec. VI we present a summary and our conclusions. In an Appendix we present the Stokes relations connecting various incident, reflected, and transmission coefficients at a single interface between an antiferromagnet and a dielectric.

II. EXAMPLES IN THE VOIGT GEOMETRY

In this section we consider examples for particular structures incorporating a uniaxial antiferromagnet in the Voigt geometry. The plane of incidence is always xy , with y normal to the interfaces, and the uniaxis of the antiferromagnet is always along z , as is the external field H_0 . In this geometry, only s -polarized radiation (E field along z) interacts with the magnetic system, and there is no mixing between polarizations. All examples are therefore in s polarization. In Fig. 1 the Voigt geometry corresponds to $\Phi = \pi/2$.

In the Voigt geometry, the magnetic permeability tensor of a uniaxial antiferromagnet at frequency ω is given by¹⁰

$$\boldsymbol{\mu} = \begin{pmatrix} \mu_1 & i\mu_2 & 0 \\ -i\mu_2 & \mu_1 & 0 \\ 0 & 0 & 1 \end{pmatrix}, \quad (2.1)$$

where

$$\mu_1 = 1 + 4\pi\gamma^2 H_a M_s (Y^+ + Y^-), \quad (2.2)$$

$$\mu_2 = 4\pi\gamma^2 H_a M_s (Y^+ - Y^-), \quad (2.3)$$

$$Y^\pm = [\omega_r^2 - (\omega \pm \gamma H_0 + i\Gamma)^2]^{-1}. \quad (2.4)$$

H_a is the anisotropy field, M_s the sublattice magnetization, γ the gyromagnetic ratio, and Γ the damping. The antiferromagnetic resonance frequency ω_r is given by

$$\omega_r = \gamma(2H_a H_e + H_a^2)^{1/2}, \quad (2.5)$$

where H_e is the exchange field.

In all the examples, we use the parameters⁴⁻⁶ for FeF_2 at 4.2 K: $M_s = 0.056$ T, $H_a = 19.745$ T, $H_e = 53.313$ T, and $\gamma = 1.05 \text{ cm}^{-1}/\text{T}$, corresponding to a bulk resonance frequency of $\omega_r = 52.45 \text{ cm}^{-1}$. The dielectric constant of the antiferromagnet is taken as 5.5. We consider examples both with $\Gamma = 0$ (zero damping and zero absorption) and with the experimentally observed value of $\Gamma = 0.05 \text{ cm}^{-1}$. We note that the low damping limit of Γ near zero is quite possible physically. Samples of MnF_2 have been reported with a damping on the order of $\Gamma = 0.001$.¹¹ For $\Gamma = 0$ both μ_1 and μ_2 are real. Otherwise they are complex. In this section we take the applied field to be $H_0 = \pm 0.5$ T.

A. Reflection off a semi-infinite antiferromagnet: Phase and amplitude behavior

We consider s -polarized reflection off a semi-infinite antiferromagnet in the Voigt geometry. The incident medium is assumed to be a dielectric (vacuum in the examples considered). For such a system the complex reflection coefficient is given by¹²

$$\tilde{r} = \frac{q_{1y}\mu_v - q_{2y} + iq_x(\mu_2/\mu_1)}{q_{1y}\mu_v + q_{2y} - iq_x(\mu_2/\mu_1)}, \quad (2.6)$$

where μ_v is the Voigt permeability given by

$$\mu_v = (\mu_1^2 - \mu_2^2)/\mu_1. \quad (2.7)$$

The electromagnetic wave in the reflection experiment is characterized by a wave vector in each medium. The component of the wave vector parallel to the surface q_x is the same in each medium and is determined by the angle of incidence:

$$q_x = \varepsilon_1(\omega/c)\sin\theta. \quad (2.8)$$

Here ε_1 is the dielectric constant of medium 1 (usually vacuum) and θ is the incident angle in a reflection experiment. The components of the wave vector perpendicular to the surface are given by q_{1y} in medium 1 and q_{2y} in medium 2 (the antiferromagnet).

$$q_{1y} = [\varepsilon_1(\omega/c)^2 - q_x^2]^{1/2}, \quad (2.9)$$

$$q_{2y} = [\varepsilon_2\mu_v(\omega/c)^2 - q_x^2]^{1/2}. \quad (2.10)$$

In discussing the nonreciprocal properties of \tilde{r} , we will find it useful to represent it in terms of an amplitude ρ and a phase ϕ :

$$\tilde{r} = \rho \exp(i\phi). \quad (2.11)$$

In order to look at nonreciprocity in \tilde{r} , we compare the results for the reflection coefficient when the incident wave travels from right to left across the magnetic field, i.e.,

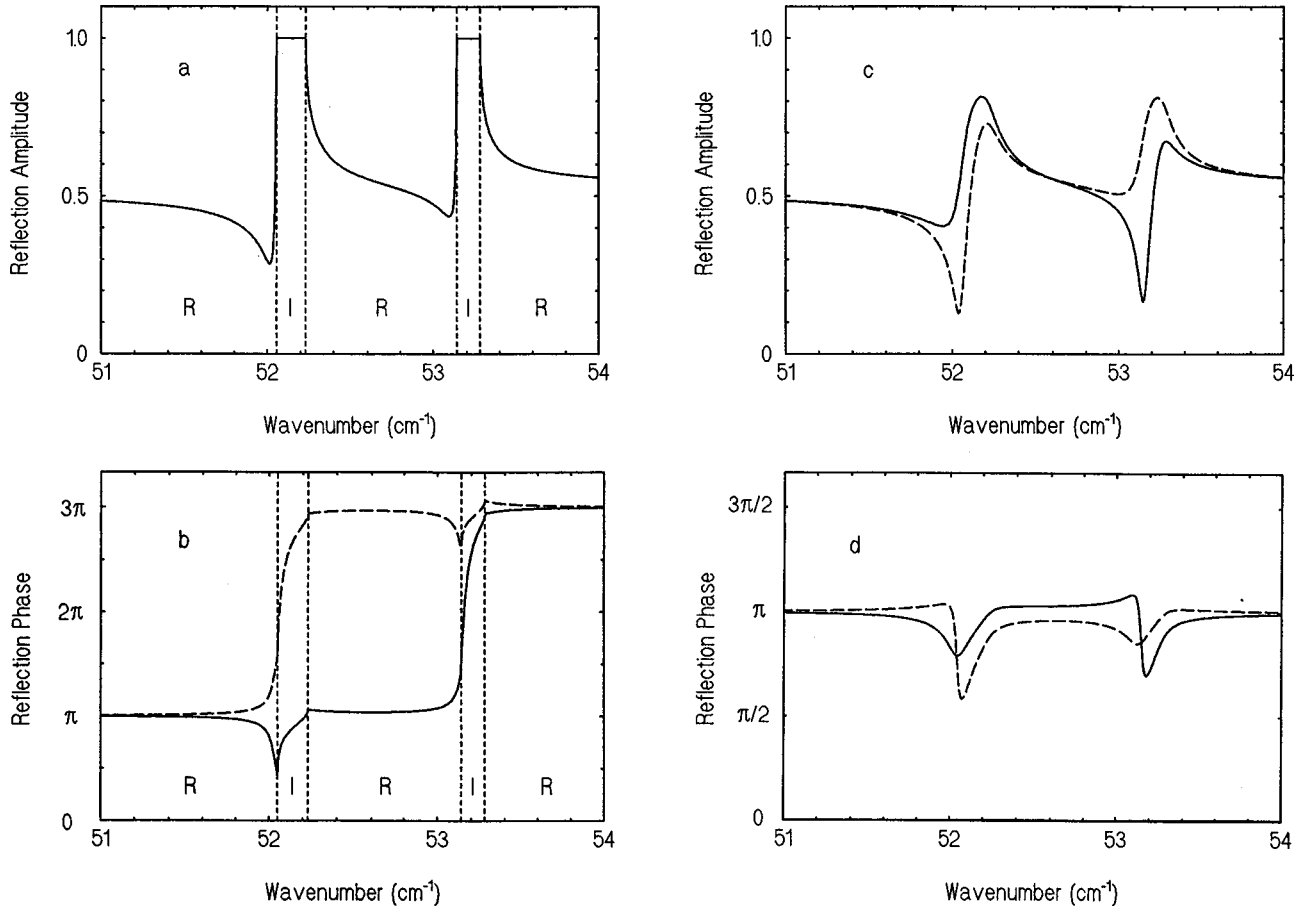


FIG. 2. Calculated amplitude and phase spectra for s -polarized reflection off a semi-infinite FeF_2 sample in the Voigt geometry in the presence of an external field of 0.5 T. (a) $\Gamma=0$, amplitude spectrum; (b) $\Gamma=0$, phase spectrum; (c) $\Gamma=0.05 \text{ cm}^{-1}$, amplitude spectrum; (d) $\Gamma=0.05 \text{ cm}^{-1}$, phase spectrum. Solid curves, $\theta = +45^\circ$; dashed curves, $\theta = -45^\circ$. Note that in the case of (a) both curves are coincident, so only a single solid curve is seen.

$\tilde{r}(+\theta)$, with those for the case where the incident wave is reversed, $\tilde{r}(-\theta)$. The geometry is illustrated in Fig. 1. The only difference between these two results arises from the fact that the sign of q_x in Eq. (2.6) is different for the two cases. We first discuss the case when the damping parameter Γ is zero, i.e., when no absorption takes place. In this case all the terms in Eq. (2.6), with the exception of q_{2y} , are real. q_{2y} may be either real or imaginary, depending on the frequency, and we consider the two cases separately.

1. q_{2y} real

This corresponds to the bulk regions of antiferromagnet, for which radiation can propagate into the sample. If we put q_{2y} real in Eq. (2.6) and separate \tilde{r} into its real and imaginary parts, we find that

$$\text{Re}[\tilde{r}(+\theta)] = \text{Re}[\tilde{r}(-\theta)], \quad (2.12)$$

$$\text{Im}[\tilde{r}(+\theta)] = -\text{Im}[\tilde{r}(-\theta)]. \quad (2.13)$$

In terms of amplitude ρ and phase ϕ , this gives

$$\rho(+\theta) = \rho(-\theta), \quad (2.14)$$

$$\phi(+\theta) = -\phi(-\theta) + 2\pi m, \quad (2.15)$$

where m is an arbitrary integer. The term $2\pi m$ is included since we find it convenient to plot phases outside the range $-\pi < \phi < \pi$. From Eqs. (2.14) and (2.15) we immediately see that while the amplitude (and thus the intensity) is reciprocal, the phase of the reflected is dramatically nonreciprocal.

2. q_{2y} imaginary

In this case the electromagnetic fields simply decay into the sample, with no propagation taking place. Calculation of the amplitude ρ from Eq. (2.6) now gives

$$\rho(+\theta) = \rho(-\theta) = 1, \quad (2.16)$$

i.e., all the radiation is reflected. The phase is nonreciprocal, but does not follow a simple symmetry relation such as given by Eq. (2.15).

In both cases above, the reflected amplitude is reciprocal but the reflected phase is nonreciprocal. If there is no damping, therefore, these results should hold throughout the spectrum. The reciprocity of the reflected amplitude is illustrated in Fig. 2(a) for the example of oblique incidence reflection off FeF_2 with $\Gamma=0$. The figure shows that the results for $\rho(+\theta)$ and $\rho(-\theta)$ are identical, confirming that the reflection amplitude is reciprocal everywhere. The regions marked R correspond to q_{2y} real, and those marked I correspond to

q_{2y} imaginary. In the latter case the reflection amplitude can be seen to be 1, in agreement with Eq. (2.16).

Figure 2(b) shows the phase spectra for the same system. Note that, in order to demonstrate the continuous change in the phase, we have shown it as varying from π to 3π over the frequency range illustrated. We have marked the regions for real and imaginary q_{2y} in the same way as for Fig. 2(a). The phase is clearly nonreciprocal in both regions. Examination shows that Eq. (2.15) is obeyed where q_{2y} is real but not where it is imaginary as expected.

From the result that the reflection amplitude r is reciprocal for zero damping, it follows that the power reflectivity $R = \bar{r}r^*$ is also reciprocal. This is a well-known result, and has also been shown by thermodynamic arguments^{3,9} as we shall discuss in Sec. IV. The nonreciprocity of the reflected phase has been commented upon in a recent review article by two of the present authors,¹² but, to our knowledge, there are no other reports of this phenomenon. We emphasize that this nonreciprocal phase has direct experimental consequences; it will prove vital in explaining the results associated with the other structures considered in this section.

We now turn to the results when damping is included. In this case the quantities μ_1 , μ_2 , μ_v , and q_{2y} in Eq. (2.6) are all complex, so the simple relationships in Eqs. (2.12)–(2.16) based on pure real or pure imaginary parameters no longer apply. Thus both the amplitude and the phase spectra are nonreciprocal, as shown in Figs. 2(c) and 2(d), respectively.

B. Reflection off a dielectric deposited on an antiferromagnet

Nonreciprocal reflectivity R from a structure consisting of a dielectric film deposited on a semi-infinite antiferromagnet has already been predicted in Ref. 13. This result can clearly be seen in Fig. 3, in which we show the overall reflectivity for a series of structures consisting of Si films ($\epsilon=11.6$) deposited on FeF_2 . We have calculated results for a series of dielectric film thicknesses, both with and without damping, using the same transfer-matrix formalism as described in Ref. 13. Of particular significance is that, in contrast to the case when the dielectric film is absent, the nonreciprocity in the reflectivity spectrum persists even in the absence of damping. Here we explain the underlying physics of such behavior in terms of interference and examine the consequent thickness dependence of the nonreciprocity. We note that the nonreciprocal phase seen in Sec. II A above will play a key role in this discussion.

The basic argument for nonreciprocal reflectivity in the absence of damping can be seen from inspection of Fig. 4. Since there are two interfaces in the structure, the overall reflectivity will be determined by interference of the reflected partial beams. A full analysis requires consideration of all the partial rays, but the reason for nonreciprocity can be seen by consideration of interference between the first two partial rays. The first of these partial rays is due to reflection off the dielectric surface (interface 1), and therefore has both reciprocal amplitude and reciprocal phase. The second partial beam, however, results from a reflection from the dielectric/antiferromagnet interface (interface 2) and has reciprocal amplitude but a *nonreciprocal* phase, as described above. Therefore the relative phase between these two partial rays must be nonreciprocal. The resulting amplitude (and hence the reflectivity) when they interfere is also nonreciprocal.

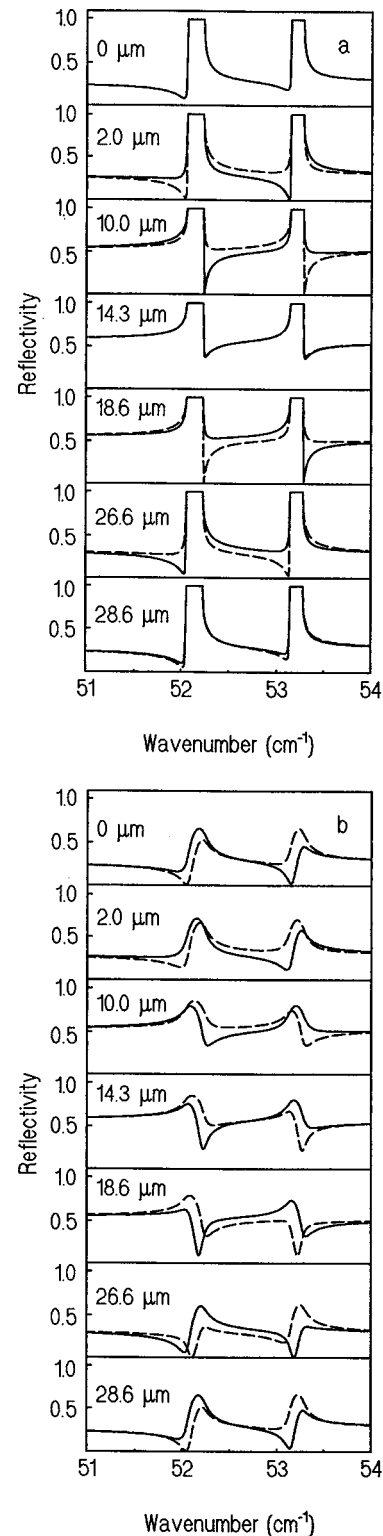


FIG. 3. Calculated reflectivity spectra for s -polarized reflection off a silicon film deposited on a semi-infinite FeF_2 sample in the Voigt geometry in the presence of an external field of 0.5 T. The results are shown for a series of film thicknesses. (a) $\Gamma=0$, (b) $\Gamma=0.05 \text{ cm}^{-1}$. Solid curves, $\theta=+45^\circ$; dashed curves, $\theta=-45^\circ$. Note that for $d=0$ in (a) both curves are coincident, so only a single solid curve is seen.

The above argument explains why, in general, reflectivity should be nonreciprocal. However, when the reflectivity off the antiferromagnet is equal to 1, then the overall reflectivity obtained from summing all the partial rays must also be 1,

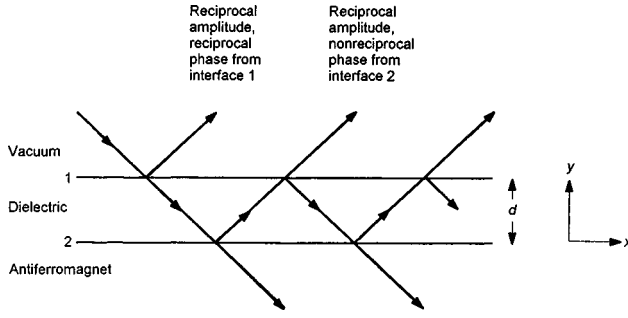


FIG. 4. Interference argument for nonreciprocal reflection in the absence of damping off a dielectric film deposited on a semi-infinite antiferromagnet.

due to conservation of energy. This occurs wherever q_{3y} is imaginary where we are now taking layer 3 to be the antiferromagnet. This is confirmed by inspection of Fig. 3(a), which shows reflectivities of 1 in the same regions as those marked *I* in Figs. 2(a) and 2(b).

Figure 3(a) shows some interesting general patterns. For instance, one can see that at a dielectric thickness of $14.3 \mu\text{m}$ the nonreciprocity in reflectivity is almost lost. As the thickness is increased, the nonreciprocity increases only to decrease again for thicker overlayers.

We may gain additional insight into the nonreciprocity by examining the reflectivity as a function of the thickness at a single frequency. The resulting plot can be understood in terms of standard Fabry-Pérot fringes that result from interference of all the reflected partial rays. Figure 5(a) shows the reflectivity at 52.03 cm^{-1} [the frequency of the low-frequency dip in Fig. 3(a)] as a function of thickness. For both $R(+\theta)$ and $R(-\theta)$ we see Fabry-Pérot fringe patterns that repeat with a period¹⁴ of

$$d_0 = \lambda_2 / (2 \cos \theta_2), \quad (2.17)$$

where λ_2 and θ_2 are the wavelength and angle of propagation, respectively, within the dielectric layer. Since, from Eq. (2.14), the individual interface reflection amplitudes for the $+\theta$ and the $-\theta$ experiments are the same, the fringe patterns are identical apart from a phase shift.

At $d=0$, the reflectivity is reciprocal (the two Fabry-Pérot curves cross), in agreement with Eq. (2.14) for reflection off a semi-infinite antiferromagnet. The curves also cross with the same reflectivity when d is a multiple of d_0 , so there is also reciprocity at these thicknesses. Since the variation in d_0 over the frequency range of interest is very small, this result applies to the overall spectra. For the numerical examples used in Figs. 3 and 5, d_0 is about $28.6 \mu\text{m}$, and we see from Fig. 3(a) that the spectra for this thickness of dielectric are indeed reciprocal.

Figure 5(a) also shows that, due to the symmetry of the Fabry-Pérot fringe pattern, the reflectivity is reciprocal at odd multiples of $d_0/2$, but it is different from that at $d=0$. The $d=14.3 \mu\text{m}$ (corresponding to $d_0/2$) result in Fig. 3(a) demonstrates this clearly.

The above results, showing reciprocity at both even and odd multiples of $d_0/2$, are special cases of a more general rule which follows from the symmetry of the Fabry-Pérot fringe patterns. Consider the reflectivities $R(+\theta)$ and $R(-\theta)$ at an arbitrary thickness $d=\delta$, less than d_0 . Then

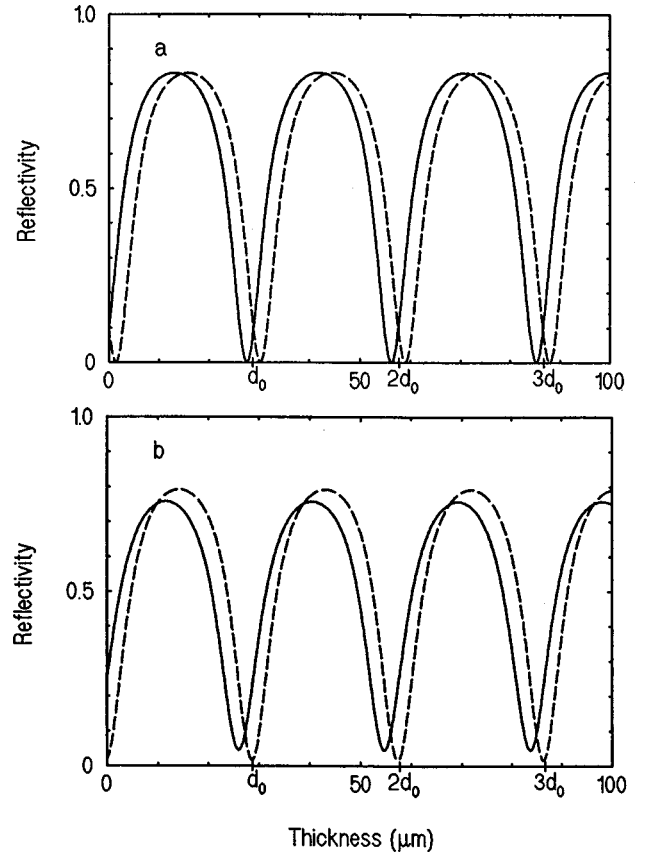


FIG. 5. Film thickness dependence of the reflectivity at a frequency of 52.03 cm^{-1} off an Si film deposited on a semi-infinite FeF_2 sample in a 0.5-T field. All conditions are the same as for Fig. 3. (a) $\Gamma=0$, (b) $\Gamma=0.05 \text{ cm}^{-1}$. Solid curves, $\theta=+45^\circ$; dashed curves, $\theta=-45^\circ$.

Fig. 5(a) shows that at a thickness of $d=d_0-\delta$ these two reflectivities will be interchanged. This can be seen over the full spectral range by comparing the spectra in Fig. 3(a) for $d=2.0 \mu\text{m}$ with those for $d=26.6 \mu\text{m}$ (i.e., $d_0-2.0 \mu\text{m}$) and those for $d=10 \mu\text{m}$ with those for $d=18.6 \mu\text{m}$ (i.e., $d_0-10 \mu\text{m}$). The rule can be trivially extended to include thicknesses greater than d_0 . Thus we see that, in principle, there is no reflectivity spectrum that is unique to either a positive or negative angle of incidence.

All the above symmetry relations can be derived formally by performing a multiple-beam analysis. Such an analysis requires the use of Stokes relations¹⁴ at the vacuum/dielectric interface and the use of Eqs. (2.14)–(2.16) at the dielectric/antiferromagnet interface.

We now briefly examine the case for which damping is present, corresponding to Figs. 3(b) and 5(b). From Fig. 5(b) we see that the Fabry-Pérot fringe pattern still has a period of d_0 , but damping has imposed a phase shift on both curves, so that they no longer cross at multiples of $d_0/2$. Thus Fig. 3(b) shows that the spectra at $d=d_0$ ($28.6 \mu\text{m}$) are the same as those at $d=0$, but they are nonreciprocal in both cases. Despite this, the two curves in Fig. 5(b) do coincide at certain values of d , suggesting that, when the dielectric has such a thickness, reciprocal reflection should occur. However, this reciprocity is unique to a particular frequency, and the overall spectrum is nevertheless nonreciprocal. This is because the phase shift imposed by the damping is highly frequency

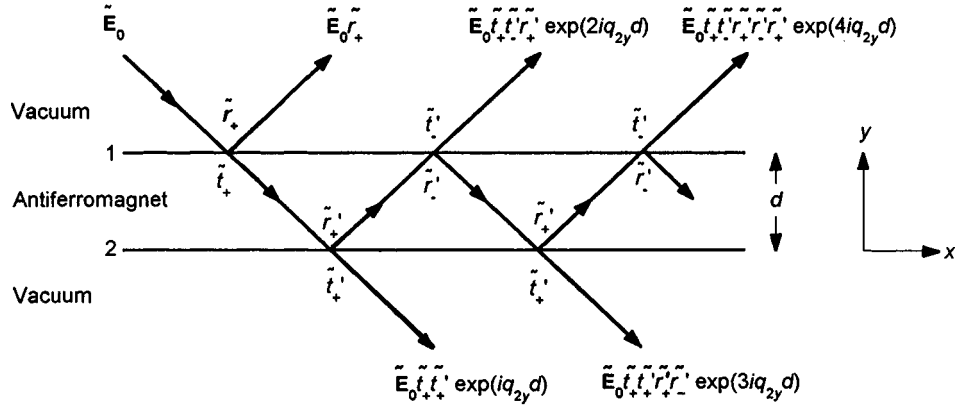


FIG. 6. Reflection and transmission coefficients, and associated partial rays, used in analyzing s -polarized reflection off and transmission through a free-standing antiferromagnet film in the Voigt geometry in the presence of an external field. The parameters are defined for an incident angle of $+\theta$. For an incident angle of $-\theta$ one would reverse the signs on the subscripts. We use the convention that a prime indicates a reflection or transmission coefficient when the incident partial wave is in the antiferromagnet.

dependent—in fact it changes sign twice over the frequency range considered. The overall spectrum is therefore never reciprocal, as observed in Fig. 3(b).

C. Transmission through and reflection off a free-standing antiferromagnetic film

Thermodynamic arguments have previously been used to show that both the reflectivity from and transmissivity through a free-standing antiferromagnetic film are reciprocal in the absence of damping.^{3,9} Here we use an interference argument to confirm and extend these results by considering both the amplitude and phase spectra for such a structure, both with and without damping.

The various reflection and transmission coefficients, defined for an angle of incidence of $+\theta$, are shown in Fig. 6. For an angle of incidence of $-\theta$, we would have to reverse the signs on all the subscripts. Note that, due to the symmetry of the structure, we can use the same coefficients, with an appropriate change of sign on the subscript, for internal reflection and transmission at interface 1 as we do at interface 2.

We first consider the case of transmission through the structure. The overall transmission coefficient can be calculated by summing partial rays. From Fig. 6 we see that, for an angle of incidence $+\theta$, the transmission coefficient is given by

$$\tilde{t}(+\theta) = \tilde{t}_+ \tilde{t}'_+ \sum_{m=0}^{\infty} (\tilde{r}'_+ \tilde{r}'_-)^m \exp[(2m+1)iq_{2y}d]. \quad (2.18)$$

In order to calculate $\tilde{t}(-\theta)$, one would merely have to interchange the signs on the subscripts. It is therefore obvious from inspection that the terms within the summation are all reciprocal, since the term $(\tilde{r}'_+ \tilde{r}'_-)$ is reciprocal (i.e., any nonreciprocity due to an internal reflection off the bottom interface is canceled by the effect of a subsequent internal reflection off the top interface).

In order to deal with the term $(\tilde{r}'_+, \tilde{t}'_+)$ outside the summation, one can make use of Stokes relations. In the Appendix, we derive an appropriate form of these relations that takes account of any nonreciprocities at the interfaces. We can combine Eqs. (A1) and (A3) to give

$$\tilde{r}_+ \tilde{t}'_+ = \tilde{r}'_- \tilde{t}'_- . \quad (2.19)$$

Substitution into Eq. (2.18) shows that the complex transmission coefficient is reciprocal, i.e., $\tilde{t}(+\theta) = \tilde{t}(-\theta)$. This shows that both amplitude and phase for transmission through a free-standing film are reciprocal, regardless of damping. We have verified this result numerically, using transfer-matrix methods,¹³ as shown in Fig. 7.

A similar analysis can be performed for reflection off the free-standing film. We then find that

$$\tilde{r}(+\theta)/\tilde{r}(-\theta) = \tilde{r}_+/\tilde{r}'_- . \quad (2.20)$$

Thus reflection off a free-standing film follows the same nonreciprocity relationships as for a semi-infinite antiferromagnet. In the case of zero damping, we therefore have reciprocal reflected amplitude but nonreciprocal reflected phase. In contrast, if damping is present, both amplitude and phase are nonreciprocal.

It also follows that any nonreciprocity in reflection, expressed as a relative amplitude $\rho(+\theta)/\rho(-\theta)$ or a phase difference $\phi(+\theta) - \phi(-\theta)$, is independent of layer thickness and is, in fact, the same as for a semi-infinite antiferromagnet. This result, which applies regardless of damping, has been verified numerically.

III. RECIPROCITY RELATIONS FOR A PLANE OF INCIDENCE AT AN ANGLE WITH RESPECT TO THE APPLIED FIELD

We now consider a geometry where the plane of incidence is not perpendicular to the applied field, i.e., the plane of incidence is still perpendicular to the surface, but is at an arbitrary angle with respect to the easy axis and the applied

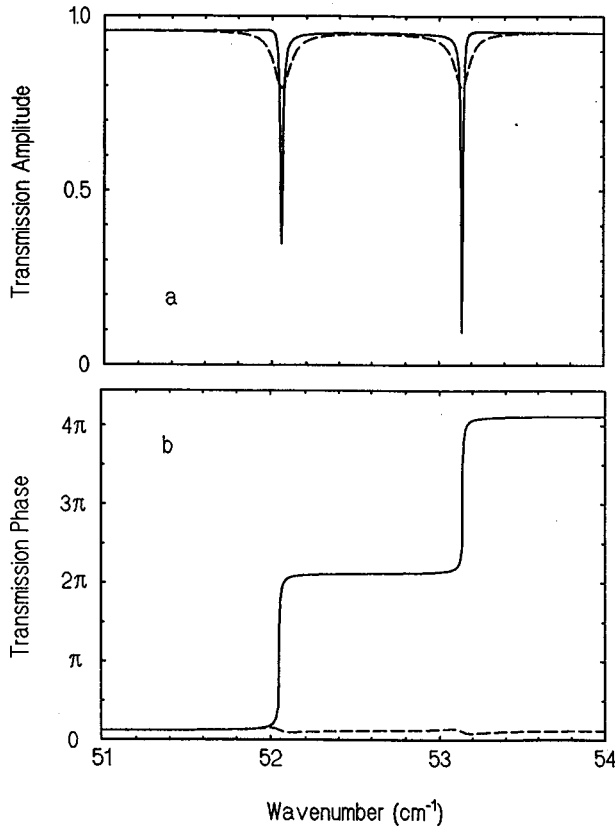


FIG. 7. Calculated amplitude and phase spectra for s -polarized transmission through a freestanding FeF_2 film in the Voigt geometry in the presence of an external field of 0.5 T. (a) Amplitude spectra, (b) phase spectra. Solid curves, $\Gamma=0$; dashed curves, $\Gamma=0.05 \text{ cm}^{-1}$. Both the transmitted amplitude and the transmitted phase are reciprocal in all cases, and each curve represents both $\theta=+45^\circ$ and $\theta=-45^\circ$ spectra.

field. In Fig. 1 this corresponds to the case where $\Phi \neq \pi/2$. In this configuration there is mode mixing, i.e., an incident wave that is s polarized gives rise to transmitted and reflected waves that are both s and p polarized. The calculation for the reflectivity and transmissivity is lengthy but is a straightforward extension of the calculation given in Ref. 9 for the semi-infinite structure, and thus we omit the details.

As an example of the general kinds of results that can be expected in this case, we present results for reflection and transmission from a $10\text{-}\mu\text{m}$ -thick antiferromagnetic film in Figs. 8 and 9. In all cases the incident wave is s polarized.

Figures 8 and 9 are for the case where the damping is $\Gamma=0.05 \text{ cm}^{-1}$. Figure 8 shows the transmitted and reflected intensities, while Fig. 9 concentrates on the transmitted and reflected phases. In Fig. 8 we see that there is significant nonreciprocity for both s - and p -polarized reflections and for p -polarized transmission. In contrast, the s -polarized transmission shows no nonreciprocity. This is, in a sense, an extension of the results found in Sec. II, i.e., with no mode mixing we found that the transmitted wave was reciprocal and that the reflected wave was not.

We examine the phase of the transmitted and reflected waves in Fig. 9. Again the nonreciprocity exists for all waves except for the transmitted s -polarized wave. It is interesting to note that the magnitude of the phase change as a function of frequency is much larger for the p -polarized waves. Fi-

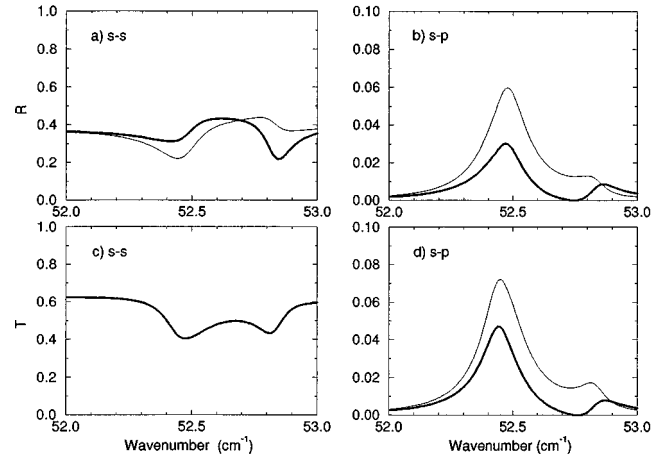


FIG. 8. Intensity for reflected and transmitted waves as a function of frequency for an antiferromagnetic film. The parameters are $H_0=1 \text{ kG}$, $d=10 \mu\text{m}$, $\Phi=35^\circ$, $\Gamma=0.05 \text{ cm}^{-1}$. The light lines are for $\theta=+30$ and the dark lines for the reversed wave are for $\theta=-30$. Only the s -to- s transmission (c) is reciprocal.

nally, we point out that we have again used the convention that the phase is not restricted to lie within the range 0 to 2π .

If the damping is zero, the symmetry properties remain the same, i.e., only the s -polarized transmission is reciprocal. The reflected and transmitted intensities and phases have the same general features seen in Figs. 8 and 9. One interesting difference is that as the damping is reduced the s to p transmission and reflection intensities get significantly larger. For example, with the damping close to zero the maximum transmitted p intensity is about 0.55.

We summarize the results of our numerical explorations as follows.

(1) The existence of nonreciprocity is independent of damping.

(2) If the incident wave is s polarized then the transmitted s -polarized wave is reciprocal in magnitude and phase. All other waves (s and p reflected waves and p transmitted

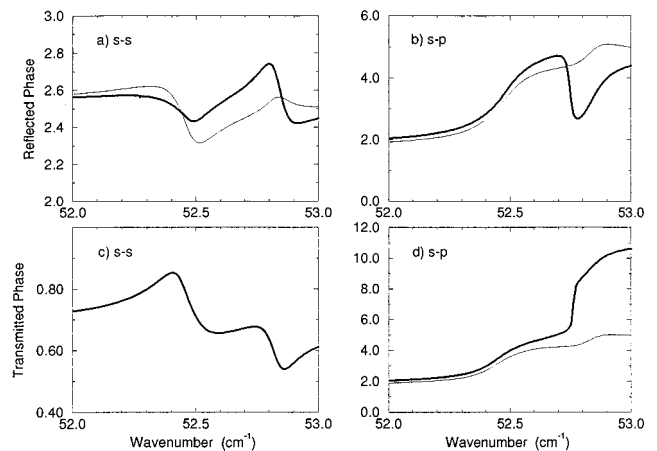


FIG. 9. Phases for the reflected and transmitted waves as a function of frequency. The parameters are $H_0=1 \text{ kG}$, $d=10 \mu\text{m}$, $\Phi=35^\circ$, $\Gamma=0.05 \text{ cm}^{-1}$. The light lines are for $\theta=+30$ and the dark lines for the reversed wave are for $\theta=-30$. Only the s -to- s transmission (c) is reciprocal.

waves) are nonreciprocal both in magnitude and phase.

(3) If the incident wave is p polarized then the transmitted p -polarized wave is reciprocal in magnitude and phase. All other waves (s and p reflected waves and s transmitted waves) are nonreciprocal both in magnitude and phase.

(4) If the incident wave is a combination of s and p polarization then nothing is reciprocal.

The relationships outlined above seem, perhaps, a bit surprising in their complexity. It is therefore of interest to see if there are any general statements that one can make about reflected and transmitted waves. In Sec. IV we do this by thermodynamic arguments.

IV. THERMODYNAMIC DISCUSSION

Apart from calculations for specific geometries, a number of arguments based on general principles have appeared. Scott and Mills¹⁵ applied symmetry methods to show that the dispersion relation for a bulk excitation must be reciprocal, but, because of the reduction of symmetry in the presence of a surface and an applied magnetic field, the dispersion relation for a surface excitation need not be.

Remer *et al.*³ used a thermodynamic analysis to discuss reflected and transmitted intensities in the Voigt geometry where the plane of incidence is perpendicular to the magnetic field. Their results will be discussed in detail below, but in brief they showed that in the Voigt geometry the reflected intensity from a semi-infinite magnetic medium is nonreciprocal only if absorption is present. In addition, they showed that in this geometry transmission through an unsupported film is always reciprocal even when absorption is present. Stamps, Johnson, and Camley⁹ were the first to consider polarization effects, but it was not relevant to their discussion to include damping. Thus one purpose of this section is to discuss nonreciprocal reflection and transmission with the inclusion of both damping and polarization. There is a need for this in light of recent work⁴⁻⁷ showing polarization mixing effects in addition to nonreciprocity for infrared reflection experiments on FeF₂.

To begin with, we emphasize that in its nature blackbody radiation is unpolarized. Part of the standard discussion^{17,18} of radiation thermodynamics involves a proof that blackbody radiation density is isotropic and independent of the nature of the cavity walls. This proof involves consideration of equilibrium between two cavities connected by a narrow-band filter F . By incorporating in F a polarization switch, e.g., a half-wave plate for circular polarizations, one can extend the proof to show that the radiation density is the same for both polarization states.

We first summarize the thermodynamics results established by Remer *et al.* The notation, essentially that of Stamps, Johnson, and Camley,⁹ is defined in Fig. 10. For a semi-infinite medium (no transmission), conservation of energy and detailed balance give

$$R(\theta) + A(\theta) = R(-\theta) + A(-\theta) = 1, \quad (4.1)$$

$$R(\theta) + E(-\theta) = R(-\theta) + E(\theta) = 1. \quad (4.2)$$

Here $R(\theta)$ is the reflected power at an angle θ as a fraction of incident power. Similar definitions hold for the absorptance $A(\theta)$ and emittance $E(\theta)$. Manipulation of these gives

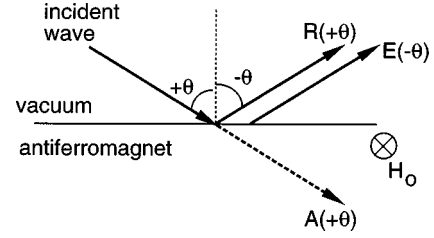


FIG. 10. Reflection geometry for thermodynamic argument on a semi-infinite sample. Reflectance $R(\theta)$ is reflected power as a fraction of incident power with similar definitions for absorptance $A(\theta)$ and emittance $E(\theta)$.

some useful results. First there is the generalized Kirchoff relation $A(\theta) = E(-\theta)$ since both of these are equal to $1 - R(\theta)$. Second, subtraction of Eq. (4.2) from Eq. (4.1) gives

$$A(\theta) + E(\theta) = A(-\theta) + E(-\theta). \quad (4.3)$$

This states that there is no momentum transfer parallel to the surface since absorptance $A(\theta)$ and emittance $E(\theta)$ are accompanied by momentum recoils $-A(\theta)$ and $-E(\theta)$.

For a thin film Eqs. (4.1) and (4.2) are replaced by

$$R(\theta) + A(\theta) + T(\theta) = R(-\theta) + A(-\theta) + T(-\theta) = 1, \quad (4.4)$$

$$R(\theta) + E(-\theta) + T(\theta) = R(-\theta) + E(\theta) + T(\theta) = 1. \quad (4.5)$$

Comparison of Eqs. (4.4) and (4.5) gives the Kirchoff relation

$$A(\theta) + T(\theta) = E(-\theta) + T(-\theta), \quad (4.6)$$

while Eq. (4.3) is replaced by

$$A(\theta) + E(\theta) + 2T(\theta) = A(-\theta) + E(-\theta) + 2T(-\theta). \quad (4.7)$$

Remer *et al.* argue that in addition Eq. (4.3) itself continues to hold for a film as a result of a distinct physics principle. Their point is that because of the variation of absorption with depth the momentum transfer is applied unevenly across the depth of the film so that the difference between the two sides of Eq. (4.3) is the momentum transfer related to the top surface and is applied to a point in the upper half of the film. This transfer, together with that from the lower surface, would exert a torque on the film and Remer *et al.* therefore assert that each transfer must vanish separately, so that Eq. (4.3) as it stands does apply for a film. Their argument is crucial since it follows immediately from Eqs. (4.3) and (4.7) that

$$T(\theta) = T(-\theta). \quad (4.8)$$

That is, the transmittance is reciprocal even if the absorptance and reflectance are nonreciprocal. This striking result has not yet been tested experimentally, but our specific calculations in the previous sections support this conclusion. In fact, this conclusion requires a bit of discussion. $T(\theta)$ above refers to unpolarized light. In our calculations we have calculated the transmitted intensity for polarized light. In the Voigt geometry, where there is no polarization mixing, the s -

and p -polarization states are independent. Thus each state must satisfy Eq. (4.8) independently. Indeed, this is what our numerical results show. When the plane of incidence is at an arbitrary angle with respect to the magnetic field, the situation discussed in Sec. III, we must first define exactly what we mean by unpolarized light before we can check on the validity of Eq. (4.8). We will do this shortly.

Our computed spectra for a film on a substrate and for a film with a dielectric overlayer show nonreciprocal transmission. We note that the above thermodynamic arguments cannot be applied for these cases or for attenuated total reflection¹⁶ since the thermodynamic arguments are based on a geometry of an unsupported film exposed to vacuum on both sides.

As pointed out above, blackbody radiation is unpolarized and thermodynamic arguments apply directly only to unpolarized radiation. However, calculations and published spectra are often for polarized input and output beams and we must therefore establish the connection between polarized spectra and the underlying thermodynamic results. This is particularly important for cases where the sample is birefringent and polarization mixing occurs in reflection and transmission. We use ideas from the elegant and general discussion of polarization given by Born and Wolf.¹⁹

It is convenient to work in terms of the usual plane polarization states s and p , partly because these have been used in experiments. We consider radiation incident at an angle θ on a film with complex s and p amplitudes given by \tilde{a}_s and \tilde{a}_p ; the corresponding intensities are $|\tilde{a}_s|^2$ and $|\tilde{a}_p|^2$. Complex coefficients \tilde{r}_{ij} are defined so that the reflected amplitudes for s polarization are given by $\tilde{r}_{ss}\tilde{a}_s + \tilde{r}_{sp}\tilde{a}_p$. Similarly, the reflected amplitudes for p polarization are given by $\tilde{r}_{ps}\tilde{a}_s + \tilde{r}_{pp}\tilde{a}_p$. Transmission coefficients t_{ij} are defined similarly. Where it is helpful we write $\tilde{r}_{ij} = \rho_{ij}\exp(i\phi_{ij})$.

Born and Wolf¹⁹ argue that the blackbody intensity, defined as an average over all polarization states, is equal to the average over two orthogonal states, say s and p . This is a key result for us since it provides the connection between the calculated reflected and transmitted intensities—which involve the individual polarizations—and the unpolarized radiation required in the thermodynamic arguments. Since we shall use this result in discussing the computed spectra, we now give an elementary proof for the reflection amplitude r_{ij} .

We consider a general polarized incident beam

$$E = (\cos \eta, \sin \eta e^{i\delta}, 0), \quad (4.9)$$

where the x and y axes for the incident beam are in the directions of s and p polarizations. The reflected beam is

$$E = (\tilde{r}_{ss}\cos(\eta) + \tilde{r}_{sp}\sin(\eta)e^{i\delta}, \tilde{r}_{ps}\cos(\eta) + \tilde{r}_{pp}\sin(\eta)e^{i\delta}, 0). \quad (4.10)$$

The reflected intensity is therefore

$$\begin{aligned} R(\eta, \delta) &= (|\tilde{r}_{ss}|^2 + |\tilde{r}_{sp}|^2)\cos^2(\eta) + (|\tilde{r}_{ps}|^2 + |\tilde{r}_{pp}|^2)\sin^2(\eta) \\ &\quad + 2 \operatorname{Re}(\tilde{r}_{ss}\tilde{r}_{sp}^*e^{-i\delta} + \tilde{r}_{ps}\tilde{r}_{pp}^*e^{-i\delta})\cos(\eta)\sin(\eta). \end{aligned} \quad (4.11)$$

The reflected intensity for incident unpolarized light is found by averaging this over η and δ :

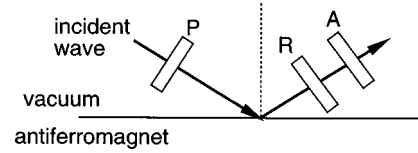


FIG. 11. Schematic of polarization experiment. P is the polarizer, R the retardation plate, and A is the analyzer.

$$\langle R \rangle = \frac{1}{2}(|\tilde{r}_{ss}|^2 + |\tilde{r}_{ps}|^2 + |\tilde{r}_{sp}|^2 + |\tilde{r}_{pp}|^2). \quad (4.12)$$

Now for s -polarized incident light $\eta=0$, and the reflected intensity is $R_s = |\tilde{r}_{ss}|^2 + |\tilde{r}_{ps}|^2$ and a similar result holds for the p intensity R_p . Comparison with Eq. (4.11) gives

$$\langle R \rangle = \frac{1}{2}(R_s + R_p) \quad (4.13)$$

as stated.

Obviously a similar result applies for transmission, i.e., the *unpolarized* transmitted intensity is given by the average of the transmitted intensity from s -polarized incident radiation and from p -polarized incident radiation. Even though the rules for the reciprocity of the individual polarizations are quite complicated, as we saw in Sec. III, our numerical calculations show that the *unpolarized* transmitted intensity is reciprocal as required by Eq. (4.8). This condition thus provides a powerful check on the accuracy of numerical calculations.

V. A METHOD TO DETERMINE RELATIVE PHASE

It is of interest to ask to what extent phase measurements are possible. The direct measurement of an absolute phase, for example, ϕ_{ss} , is a difficult task, though not impossible in principle. On the other hand, phase differences like $\phi_{ps} - \phi_{ss}$ should be measurable with fairly simple modifications of existing instruments.

As far as measurement of ϕ_{ss} , say, is concerned, it is sufficient to consider a case with no polarization mixing, and therefore an incident s beam produces only a reflected s beam. To find the phase ϕ_{ss} of the latter relative to the former involves a technique like dispersive Fourier-transform spectroscopy (DFTS) in which the reflection takes place within the interferometer itself. DFTS has been established for normal-incidence reflection in zero magnetic field²⁰ but the development for oblique incidence in a non-zero field would be a formidable task.

The phase differences, on the other hand, can be found by adding a polarizer in the incident beam and analyzer in the output beam and making a number of measurements with different settings of the polarizer and analyzer. We discuss the arrangement shown in Fig. 11. A retardation plate assumed to retard the y amplitude by ε relative to the x amplitude is included; it is not strictly necessary but might prove useful in practice. When the polarizer is set an angle η and the analyzer at an angle θ , the incident beam is $(\cos(\eta), \sin(\eta), 0)$ and the reflected beam has the following amplitude along its polarization direction:

$$\begin{aligned} E(\eta, \theta, \varepsilon) &= (\tilde{r}_{ss}\cos \eta + \tilde{r}_{sp}\sin \eta)\cos \theta \\ &\quad + (\tilde{r}_{ps}\cos \eta + \tilde{r}_{pp}\sin \eta)e^{i\varepsilon}\sin \theta. \end{aligned} \quad (5.1)$$

The intensity $I = |E|^2$ is therefore

$$\begin{aligned}
I(\eta, \theta, \varepsilon) = & [\rho_{ss}^2 \cos^2 \eta + \rho_{sp}^2 \sin^2 \eta + 2\rho_{ss}\rho_{sp} \cos(\phi_{ss} - \phi_{sp}) \cos \eta \sin \eta] \cos^2 \theta \\
& + [\rho_{ps}^2 \cos^2 \eta + \rho_{pp}^2 \sin^2 \eta + 2\rho_{ps}\rho_{pp} \cos(\phi_{pp} - \phi_{ps}) \cos \eta \sin \eta] \sin^2 \theta \\
& + 2\rho_{ss}\rho_{ps} \cos(\phi_{ss} - \phi_{ps} - \varepsilon) \cos^2 \eta \sin \theta \cos \theta + 2\rho_{ss}\rho_{pp} \cos(\phi_{ss} - \phi_{pp} - \varepsilon) \cos \eta \sin \eta \sin \theta \cos \theta \\
& + 2\rho_{sp}\rho_{ps} \cos(\phi_{sp} - \phi_{ps} - \varepsilon) \cos \eta \sin \eta \sin \theta \cos \theta + 2\rho_{sp}\rho_{pp} \cos(\phi_{sp} - \phi_{pp} - \varepsilon) \sin^2 \eta \sin \theta \cos \theta. \quad (5.2)
\end{aligned}$$

The quantities to be measured are the four amplitudes ρ_{ss} , etc., and three phase differences $\phi_{ss} - \phi_{sp}$, etc. It is clear that these can be measured with no retardation plate $\varepsilon=0$ and that there are many possible combinations of η and θ that can be used to obtain the amplitudes and the phase differences. As an illustration, we display a simple set:

$$I(0,0,0) = \rho_{ss}^2, \quad (5.3)$$

$$I\left(\frac{\pi}{2}, 0, 0\right) = \rho_{sp}^2, \quad (5.4)$$

$$I\left(0, \frac{\pi}{2}, 0\right) = \rho_{ps}^2, \quad (5.5)$$

$$I\left(\frac{\pi}{2}, \frac{\pi}{2}, 0\right) = \rho_{pp}^2, \quad (5.6)$$

$$I\left(\frac{\pi}{4}, 0, 0\right) = \frac{1}{2}[\rho_{ss}^2 + \rho_{sp}^2] + \rho_{ss}\rho_{sp} \cos(\phi_{ss} - \phi_{sp}), \quad (5.7)$$

$$I\left(\frac{\pi}{4}, \frac{\pi}{2}, 0\right) = \frac{1}{2}[\rho_{ps}^2 + \rho_{pp}^2] + \rho_{ps}\rho_{pp} \cos(\phi_{pp} - \phi_{ps}), \quad (5.8)$$

$$I\left(0, \frac{\pi}{4}, 0\right) = \frac{1}{2}[\rho_{ss}^2 + \rho_{ps}^2] + \rho_{ss}\rho_{ps} \cos(\phi_{ss} - \phi_{ps}). \quad (5.9)$$

It is clear that seven measurements are required to measure the complete set of seven unknowns. We note that although the retardation plate is not necessary in principle, its inclusion might increase accuracy of some phase determinations.

VI. SUMMARY AND CONCLUSIONS

In this paper we have explored the properties of the transmitted and reflected waves when an electromagnetic wave is incident on a variety of structures containing an antiferromagnet. In particular, we have pointed out that the phase of the reflected wave off a semi-infinite antiferromagnet may be nonreciprocal even when the intensity of the reflected wave is reciprocal. This nonreciprocal phase has direct and measurable consequences when a dielectric overlayer is added above the antiferromagnet in that the intensity and phase both become nonreciprocal. The behavior of the transmitted wave, in contrast, is often reciprocal (both in ampli-

tude and phase) even when the reflected is completely nonreciprocal.

We point out that the previous symmetry arguments only suggest that the dispersion relation *can be* nonreciprocal in certain geometries. This applies equally well to oblique incidence reflection and therefore these symmetry arguments indicate that the phase can also be nonreciprocal. In contrast, the thermodynamic arguments require reciprocity of the intensity in some situations (when absorption is not present, for example), but this says nothing about the phase. Thus phase nonreciprocity may be expected in situations where the reflected intensity is reciprocal. In this paper we give examples of such a situation.

We have concentrated in this paper on discussing experiments that could be performed in a Fourier-transform infrared (FTIR) system since this gives complete information about the behavior of the reflectivity as a function of frequency. In addition, the FTIR method has been used recently to obtain results on FeF₂. However, one could envision other possible techniques. For example, an infrared laser at a single frequency could be used. This might allow a simpler determination of relative phase. For example, the initial laser beam could be split, with one beam hitting the sample and the other hitting a mirror with well-known reflection charac-

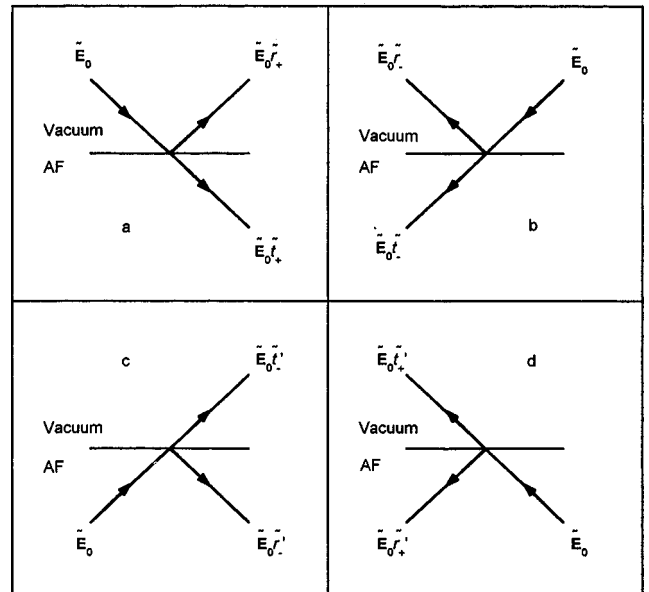


FIG. 12. Reflection and transmission coefficients used in deriving Stokes relations in the presence of nonreciprocal reflection. We use the convention that a prime indicates a reflection or transmission coefficient when the incident partial wave is in the antiferromagnet. The plus and minus subscripts indicate the direction of the incident wave.

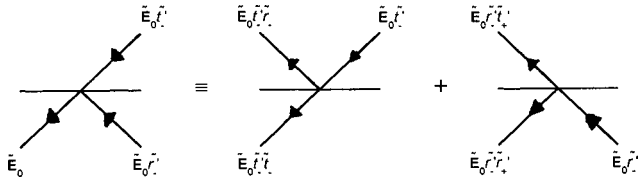


FIG. 13. Analysis used in deriving Eqs. (A1) and (A2), based on applying the principle of reversibility of light to Fig. 12(c).

teristics. The two beams could then be combined, and the interference of the two beams measured. The disadvantage of this technique, of course, is that it is restricted to a single frequency.

We note that the behavior explored in this paper should be a general feature in many magnetic systems, not just in antiferromagnets. The gyrotropic form of the permeability tensor in Eq. (2.1) is common to ferromagnets, antiferromagnets, and weak ferromagnets. The frequency region where this nonreciprocity can be explored, however, will vary considerably depending on the material. It is interesting to note that doped semiconductors in a magnetic field can also show nonreciprocal reflection of intensities. In this case it is because the dielectric tensor acquires a gyrotropic form,¹ with imaginary off-diagonal elements. It would be reasonable to expect that these systems also would display nonreciprocal reflection in phase under similar circumstances, and this should be investigated in the future.

The fact that both the intensity and the phase of the transmitted wave in the Voigt geometry are reciprocal is quite interesting. One might try to explain this using a symmetry argument. For example, in the absence of a magnetic field the reflection of the system through the yz plane is a symmetry operation. This operation effectively reverses the direction of propagation parallel to the surfaces. However, since it is a symmetry operation, it requires that the transmission be reciprocal both in phase and in intensity.

The situation is quite different when a magnetic field is applied in the plane of the surface. The reflection through the yz plane is no longer a symmetry operation since it reverses the external magnetic field at the same time as the direction of propagation. One can consider a variety of operations involving time reversal. For example, time reversal followed by a reflection in the yz plane is a symmetry operation for the system, as is time reversal followed by a reflection about the midplane of the film. Unfortunately, we could not find any combination of symmetry operations that related the field configuration for propagation with $+\theta$ to the appropriate field configuration with $-\theta$. Thus a symmetry discussion does not seem to be able to amplify this result.

ACKNOWLEDGMENTS

The work of R.E.C. was supported by ARO Grant No. DAAH04-94-G-0253 and by EPSRC. T.D. was supported by

the Brazilian agency CAPES. The work at USM was supported by IRPA (Malaysian Government) Grant No. 09-02-05-6001. We appreciate helpful discussions with Professor T. J. Parker and Professor S. R. P. Smith.

APPENDIX: STOKES RELATIONS IN THE PRESENCE OF NONRECIPROCAL REFLECTION

Here we extend the standard form of Stokes relations¹⁴ to an interface at which nonreciprocal reflection occurs, e.g., a vacuum/antiferromagnetic interface. We consider the case when there is no mixing of polarizations (as in the Voigt geometry) and no damping.

We consider all quantities in terms of E fields, and define the complex reflection and transmission coefficients shown in Fig. 12. We now apply time reversal, which causes a change of sign in both ω and H_0 . Inspection of Eq. (4) shows that, for $\Gamma=0$, this leaves the permeability unchanged. Application of the time reversal to any of the diagrams in Fig. 12 therefore simply amounts to reversing the signs of all the arrows.

Figure 13 shows what happens when we reverse the arrows of Fig. 12(c), i.e., the result of a ray with complex field $E_0\tilde{r}'_-$ entering from the top right simultaneously with a ray with complex field $E_0\tilde{r}'_-$ from the bottom right. We can use Figs. 12(b) and 12(d) to work out the reflected and transmitted fields associated with each of these two incident rays, as shown explicitly in Fig. 13. According to the figure, therefore, the field associated with the overall emergent ray may be regarded as the sum of two fields, each due to an individual incident ray. The total field emerging from the bottom left is E_0 , so we get (after canceling out the E_0 's)

$$1 = \tilde{t}'_- \tilde{t}'_- + \tilde{r}'_- \tilde{r}'_+ . \quad (\text{A1})$$

Since there is no ray emerging from the top left, we also have (making the same cancellation)

$$0 = \tilde{t}'_- \tilde{r}'_- + \tilde{r}'_- \tilde{t}'_+ . \quad (\text{A2})$$

If we perform the same procedure based on reversing the arrows in Fig. 12(d) we get the equations

$$1 = \tilde{t}'_+ \tilde{t}'_+ + \tilde{r}'_+ \tilde{r}'_+ , \quad (\text{A3})$$

$$0 = \tilde{t}'_+ \tilde{r}'_+ + \tilde{r}'_+ \tilde{t}'_+ . \quad (\text{A4})$$

The above equations may be combined to produce the required relationships. A further four equations may be obtained by reversing the arrows in Figs. 12(a) and 12(b), but they are not required for the analysis presented in this paper.

The above analysis applies for zero damping. However, the expressions for reflection and transmission coefficients in the Voigt geometry satisfy Eqs. (A1)–(A4) regardless of damping.

*Permanent address: UFRN, Departamento de Física, Caixa Postal 1641, 59072-970 Natal RN, Brazil.

†Permanent address: Département of Physics, University of Colorado at Colorado Springs, Colorado Springs, CO 80933-7150.

‡Permanent address: Jurusan Fisika FMIPA, Universitas Gadjah Mada, Yogyakarta 55281, Indonesia.

§Permanent address: School of Physics, Universiti Sains Malaysia, 11800 USM Penang, Malaysia and Department of Physics, Uni-

versity of Essex, Colchester C04 3SQ, United Kingdom.

- ¹See the review article on nonreciprocity by R. E. Camley, *Surf. Sci. Rep.* **7**, 103 (1987).
- ²L. Remer, B. Lüthi, H. Sauer, R. Geick, and R. E. Camley, *Phys. Rev. Lett.* **56**, 2752 (1986).
- ³L. Remer, E. Mohler, W. Grill, and B. Lüthi, *Phys. Rev. B* **30**, 3277 (1984).
- ⁴D. E. Brown, T. Dumelow, T. J. Parker, Kamsul Abraha, and D. R. Tilley, *Phys. Rev. B* **49**, 12 266 (1994).
- ⁵Kamsul Abraha, D. E. Brown, T. Dumelow, T. J. Parker, and D. R. Tilley, *Phys. Rev. B* **50**, 6808 (1994).
- ⁶M. R. F. Jensen, T. J. Parker, Kamsul Abraha, and D. R. Tilley, *Phys. Rev. Lett.* **75**, 3756 (1995).
- ⁷M. R. F. Jensen, S. A. Feiven, T. J. Parker, and R. E. Camley, *Phys. Rev. B* **55**, 2745 (1997).
- ⁸P. Grünberg, in *Light Scattering in Solids V*, edited by M. Cardona and G. Guntherodt (Springer, Berlin, 1989); C. E. Patton, *Phys. Rep.* **103**, 251 (1984).
- ⁹R. L. Stamps, B. L. Johnson, and R. E. Camley, *Phys. Rev. B* **43**, 3626 (1991).
- ¹⁰D. L. Mills and E. Burstein, *Rep. Prog. Phys.* **37**, 817 (1974).
- ¹¹R. W. Sanders, D. Pagnette, V. Jaccarino, and S. M. Rezende, *Phys. Rev. B* **10**, 132 (1974).
- ¹²Kamsul Abraha and D. R. Tilley, *Surf. Sci. Rep.* **24**, 129 (1996).
- ¹³T. Dumelow and R. E. Camley, *Phys. Rev. B* **54**, 12 232 (1996).
- ¹⁴See, for instance, F. L. Pedrotti and L. S. Pedrotti, *Introduction to Optics*, 2nd ed. (Prentice-Hall, Englewood Cliffs, 1993).
- ¹⁵R. Q. Scott and D. L. Mills, *Phys. Rev. B* **15**, 3545 (1977).
- ¹⁶R. E. Camley and D. L. Mills, *Phys. Rev. B* **26**, 1280 (1982).
- ¹⁷A. Sommerfeld, *Optics* (Academic, New York, 1956).
- ¹⁸C. J. Adkins, *Equilibrium Thermodynamics* (Cambridge University Press, New York, 1983).
- ¹⁹M. Born and E. Wolf, *Principles of Optics* (Pergamon, New York, 1975).
- ²⁰T. J. Parker, *Contemp. Phys.* **31**, 335 (1990).